X-Ray Characterization of glass fiber reinforced thermoplastic orientation and fatigue damage evolution for automotive technical part

H. Nouri[a,b*], A. Ayadi[a,b], F. Roger[a,b], H. Maitournam[c], S. Guessasma[d], I. Raoult[e]

[a] *Mines Douai, Department of Polymers and Composites Technology and Mechanical Engineering, 941 rue Charles Bourseul, CS 10838, F-59508 Douai Cedex, France*
[b]*Univ. Lille Nord de France, F-59000 Lille, France*
[c]*Mechanical Engineering Unit, Materials and Structures group, ENSTA-ParisTech, 91762 Palaiseau, France.*
[d]*Bioengineering lab, Department of Engineering, University of Cambridge, Trumpington Street Cambridge CB2 1PZ, United Kingdom.*
[e]*PSA Peugeot Citroën (Direction Scientifique et des Technologies futures), Route de Gisy, 78943 Vélizy-Villacoublay, cedex, France*
**hedi.nouri@mines-douai.fr*

Keywords: X-ray tomography, glass fiber reinforced thermoplastics, fatigue damage model, Identification.

Abstract

The current work presents a new contribution to the phenomenological modeling of mechanical fatigue damage in short glass fiber reinforced thermoplastic matrix composites for PA66-GF35. The majority of Injection Simulation Softwares are not able to predict a realistic orientation and repartition of fibers in the corner or flange of complex component such as in the automotive parts. The first part of this work is to implement the experimental distribution of short glass fiber in order to simulate realistic fatigue damage for GFRP. For this reason, Micro X-ray tomography is used to characterize the repartition and the orientation of glass fiber in critical area of the automotive part (flange, corner ...).

The fatigue damage model used in this work is developed by Nouri et al [1]. (NML) in order to simulate the fatigue damage in glass fiber reinforced plastics GFRP. This model is able to predict the three damage stages observed during cycling loading of thermoplastics composite reinforced by glass fiber: i) onset of the damage, ii) coalescence of microcracks and propagation, iii) macroscopic cracks propagation and material failure. Glass fiber orientation and repartition obtained by X-ray tomography is used to create Abaqus cae file for automotive part. The model is implemented via Umat into Abaqus. The model parameters are identified using an inverse strategy with one single specimen based on heterogeneous fatigue tests. It consists on the use of optical whole-field displacement/strain measurements (digital image correlation) coupled to an inverse method from one single coupon. It is worth noting that the mechanical test must give rise to heterogeneous stress/strain fields. Indeed, in this case, the constitutive parameters are expected to be all involved in the response of the specimen.

1. Introduction

For reinforced thermoplastics, safety against fatigue damage is considered as the decisive factor for an optimum part design. However, the optimal design must be assessed with a

minimum of expensive prototype testing. To reach this goal, material and structural analysis must be carried-out by numerical simulation to monitor stresses field evolution and damage accumulation during cyclic loading.

The micro-mechanisms of damage accumulation occur sometimes independently and sometimes interactively, and the predominance of one or other of them may be strongly affected by both material variables and testing conditions. In case of composite materials, the damage is characterised by the material irreversible degradations. The basic modes of the material degradation have been studied and modelled in case of static [1–3] and cyclic loads [4, 5]. The damage consists mainly in the onset, the coalescence and the propagation of matrix micro-cracks, interface debonding and fiber breakage. For cyclic loading, composite materials may exhibit a stiffness reduction beginning at the first cycle. It increases progressively leading to macroscopic failure.

In glass fiber reinforced composites subjected to cyclic loading, it appears that the damage evolution occurs according to three stages [6]:

Stage 1: This stage corresponds to the onset of ‘‘damage zones”, which contain matrix micro cracks and other forms of damage, such as matrix micro-voids. Hence, damage starts very early after a low number of loading cycles. It gives rise to an initial high stiffness reduction of the composite material, notably for low and moderate levels of imposed load or displacement.

Stage 2: This stage corresponds to the coalescence and the propagation of the micro-discontinuities created during the first stage. The propagation occurs notably at the fiber–matrix interface zones. A gradual stiffness reduction of the material is then observed. This stage is a behaviour accommodation and is characterised by a relative steady reduction of the composite stiffness as a function of cycle number.

Stage 3: It corresponds to the last stage and is characterised by a dramatic damage accumulation due to the appearing of fiber fracture and macroscopic cracks propagation. The third damage stage may result in a rapid stiffness reduction leading to the total material failure.

The proposed model is built in the framework of the continuum damage mechanics using an incremental description of the anisotropic damage evolution. This formulation could be useful to predict the anisotropic damage evolution under multiaxial cyclic load and even with variable amplitude.

In the present work, the damage model has been numerically implemented into the FE software Abaqus. This has been performed to predict the fatigue damaged behaviour of injected short glass fiber reinforced polyamide.

The numerical simulation results for damage evolution is based on the tomography X-Ray of short glass fiber distribution and orientation in the thickness of sample.

2. Fatigue damage model

To take into account the observed three damage stages, a new polycylic fatigue damage model is formulated on the basis of the meso model proposed by Ladevèze and Ledantec [6]. According to the continuum damage mechanics, the damage is introduced as an internal state variable coupled to elastic behaviour. Assuming a thin structure where $\sigma_{33}=0$, made of an orthotropic material, elastic moduli of the damaged material are given by:

$$\begin{aligned} E_{11} &= E_{11}^0\left(1-d_{11}\right) \\ E_{22} &= E_{22}^0\left(1-d_{22}\right) \\ G_{12} &= G_{12}^0\left(1-d_{12}\right) \\ G_{13} &= G_{13}^0\left(1-d_{13}\right) \\ G_{23} &= G_{23}^0\left(1-d_{23}\right) \end{aligned} \tag{1.1}$$

where E_{11} (resp. E_{22}) is the Young's modulus in the longitudinal (resp. transverse) direction. G_{12}, G_{13} and G_{23} are the shear moduli. d_{ij} are the damage variables associated to the corresponding moduli. The superscript 0 indicates initial values measured when d_{ij}=0. In the case where damage is disregarded, the elastic strain energy (W_e) is given by:

$$\begin{aligned} W_e = \frac{1}{2}\frac{1}{1-\nu_{12}\nu_{21}}&\left[\left[E_{11}^0\varepsilon_{11}+\nu_{21}E_{11}^0\varepsilon_{22}\right]\varepsilon_{11}+\left[\nu_{12}E_{22}^0\varepsilon_{11}+E_{22}^0\varepsilon_{22}\right]\varepsilon_{22}\right] \\ &+G_{12}^0\gamma_{12}^2+G_{13}^0\gamma_{13}^2+G_{23}^0\gamma_{23}^2 \end{aligned} \tag{1.2}$$

For a damaged material, the elastic strain energy becomes dependent on the state variables d_{ij}. Then, the strain energy (W_d) of a damaged material can be computed from Eq.(1.2) by replacing (E_{ij}^0, G_{ij}^0) by the corresponding moduli (E_{ij}, G_{ij}) expressed in Eq. (1.1). One obtains:

$$\begin{aligned} W_d = &\frac{1}{2}\frac{1}{1-\nu_{12}\nu_{21}}\left[E_{11}^0(1-d_{11})\varepsilon_{11}\left\langle\varepsilon_{11}+\nu_{21}\varepsilon_{22}\right\rangle_+ + E_{11}^0\varepsilon_{11}\left\langle\varepsilon_{11}+\nu_{21}\varepsilon_{22}\right\rangle_-\right] \\ &+\frac{1}{2}\frac{1}{1-\nu_{12}\nu_{21}}\left[E_{22}^0(1-d_{22})\varepsilon_{22}\left\langle\varepsilon_{22}+\nu_{12}\varepsilon_{11}\right\rangle_+ + E_{22}^0\varepsilon_{22}\left\langle\varepsilon_{22}+\nu_{12}\varepsilon_{11}\right\rangle_-\right] \\ &+G_{12}^0(1-d_{12})\gamma_{12}^2+G_{13}^0(1-d_{13})\gamma_{13}^2+G_{23}^0(1-d_{23})\gamma_{23}^2 \end{aligned} \tag{1.3}$$

where (<A>+) and (<A>-) stand for the positive and negative parts of A, respectively. Thus, the damage affects E_{11} (resp. E_{22}) only when $\varepsilon_{11}+\nu_{21}\varepsilon_{22}$ (resp. $\varepsilon_{11}+\nu_{21}\varepsilon_{22}$) is positive. This can be explained by the following. When the material is submitted to a compressive loading, transverse matrix cracks are supposed to be closed up and do not have any effect on the damage evolution. On the opposite, during tension loading those cracks are active and contribute to the development of the damage.

The thermodynamic dual variables Y_{ij} associated to the damage variables d_{ij} are deduced from the elastic strain energy W_d of the degraded material:

$$\begin{aligned} Y_{11} &= -\frac{\partial W_d}{\partial d_{11}} = \frac{1}{2}\frac{1}{1-\nu_{12}\nu_{21}}E_{11}^0\varepsilon_{11}\left\langle\varepsilon_{11}+\nu_{21}\varepsilon_{22}\right\rangle_+ & Y_{12} &= -\frac{\partial W_d}{\partial d_{12}} = \frac{1}{2}G_{12}^0\gamma_{12}^2 \\ Y_{22} &= -\frac{\partial W_d}{\partial d_{22}} = \frac{1}{2}\frac{1}{1-\nu_{12}\nu_{21}}E_{22}^0\varepsilon_{22}\left\langle\varepsilon_{22}+\nu_{12}\varepsilon_{11}\right\rangle_+ & Y_{13} &= -\frac{\partial W_d}{\partial d_{13}} = \frac{1}{2}G_{13}^0\gamma_{13}^2 \\ & & Y_{23} &= -\frac{\partial W_d}{\partial d_{23}} = \frac{1}{2}G_{23}^0\gamma_{23}^2 \end{aligned} \tag{1.4}$$

In the proposed modelling, the damage rate is assumed to be the sum of two components:

$$\frac{d(d_{11})}{d(N)} = \frac{\alpha_{11}\beta_{11}}{1+\beta_{11}}\left(Y_{11}\right)^{\beta_{11}-1} + \lambda_{11}\left(Y_{11}\right)\left(e^{-(\delta_{11}N)}\right) \tag{1.5}$$

$$\frac{d(d_{22})}{d(N)} = \frac{\alpha_{22}\beta_{22}}{1+\beta_{22}}\left(Y_{22}\right)^{\beta_{22}-1} + \lambda_{22}\left(Y_{22}\right)\left(e^{-(\delta_{22}N)}\right) \tag{1.6}$$

$$\frac{d(d_{12})}{d(N)} = \frac{\alpha_{12}\beta_{12}}{1+\beta_{12}}\left(Y_{12}\right)^{\beta_{12}-1} + \lambda_{12}\left(Y_{12}\right)\left(e^{-(\delta_{12}N)}\right) \tag{1.7}$$

$$\frac{d(d_{13})}{d(N)} = \frac{\alpha_{13}\beta_{13}}{1+\beta_{13}}\left(Y_{13}\right)^{\beta_{13}-1} + \lambda_{13}\left(Y_{13}\right)\left(e^{-(\delta_{13}N)}\right) \tag{1.8}$$

$$\frac{d(d_{23})}{d(N)} = \frac{\alpha_{23}\beta_{23}}{1+\beta_{23}}\left(Y_{23}\right)^{\beta_{23}-1} + \lambda_{23}\left(Y_{23}\right)\left(e^{-(\delta_{23}N)}\right) \tag{1.9}$$

The first contribution, scaled by $(Y_{ij})^{\beta ij-1}$ in Eqs. (1.5) to (1.9), is derived from the Norton dissipation potential. Note that in a previous work from Sedrakian et al [1], the damage evolution is only described by this first term. The second component is introduced in order to describe the rapid stiffness reduction occurring during cyclic loading of reinforced thermoplastics. The developed model is then a complete model in the sense that the entire damage process (3 stages) could be described. The instantaneous state variables $d_{ij}(N)$ are obtained by numerical integration of Eqs. (1.5) to (1.9), with the initial conditions $d_{ij}(N=0)=d^{qs}{}_{ij}$. These initial values are function of the imposed displacement. In the case where the applied strain $\varepsilon^{app}{}_{ij}$ is below a threshold value associated to the beginning of the damage process in the (i,j) direction, $d^{qs}{}_{ij}=0$. From Eqs. (1.5) to (1.9), it appears that the proposed model involves 20 parameters in the general case of a 3 –D structure. Nevertheless, it should be mentioned that the model is essentially developed for thin composite structures. In that particular case, relationships governing the damage evolution are reduced to Eqs. (1.5) to (1.7) and only 12 parameters have to be identified namely, 4 parameters per damage variable. In the precedent work the 12 parameters are identified. In the next section we describe the experimental procedure of our study.

3. Experimental procedure

3.1 Material and samples

The material of this study is PA66GF35. The trade name is Zytel® 70G35 HSLX. This material contains a short glass fiber weight fraction of 35%. Fibers have a nominal diameter of 10 µm and an average fiber length, after injection moulding, of 250 µm. Conventional material data are compiled in Table 1.

	Matrix (PA6.6)	E-glass fiber
Young Modulus (MPa)	1987	72,000
Poisson coef. (-)	0.4	0.22
Density (kg/m^3)	1.16	2.54

Table 1. Elastic properties of polyamide 6.6 matrix and glass fiber

In order to investigate the influence of the fiber orientation distribution in the thickness, a notched fatigue sample is chosen. This sample (Figure 1) is obtained by injection from one side gate situated in the bottom left corner as shown in Figure 1.
The distribution of fiber is affected by the geometrical accident and by the gate location. The heterogeneous skin-core flow during injection affects the fiber orientation in the thickness. The glass fiber distribution and orientation is determined by X-Ray Tomography in the thickness of this sample for several sections of undamaged and damaged samples. Figure 2 shows the X-Ray Tomography system and corresponding micro CT.

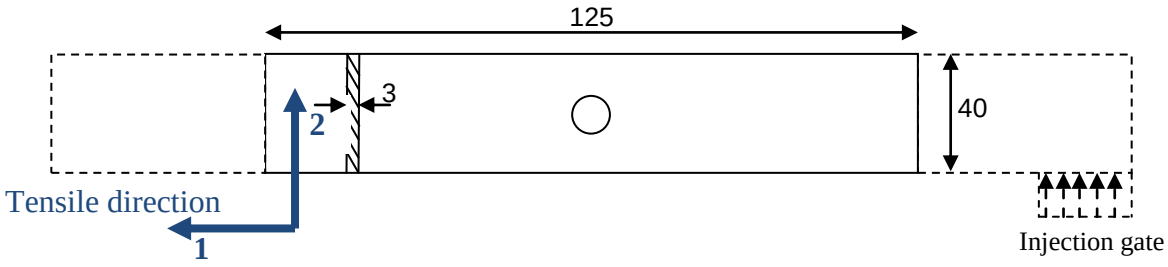

Figure 1: Specimen used for fatigue tension tests (dimensions in mm).

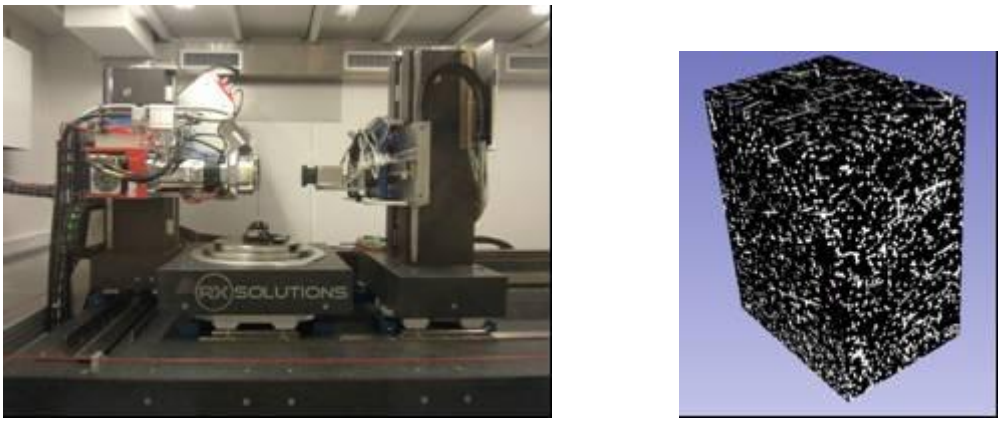

(a) (b)

Figure 2. (a) X-Ray Tomography System, (b) Typical Short glass fiber distribution in the thickness of the notched sample.

3.2 Experimental procedure

Fatigue tests were stress controlled under tension-tension mode, with a stress ratio of R=0.1 and carried out using a servo-hydraulic machine. The imposed load wave was sinusoidal with constant amplitude. **T**he frequency of 2 Hz was chosen in order to avoid a global heat of the sample. All tests were performed at room temperature. The mechanical properties of the material have been extracted from static tension tests.

4. Results and discussion

Figure 3 shows a comparison between the experimental strain fields and numerical strain fields after 2000 cycles. These results are obtained by a fatigue test.

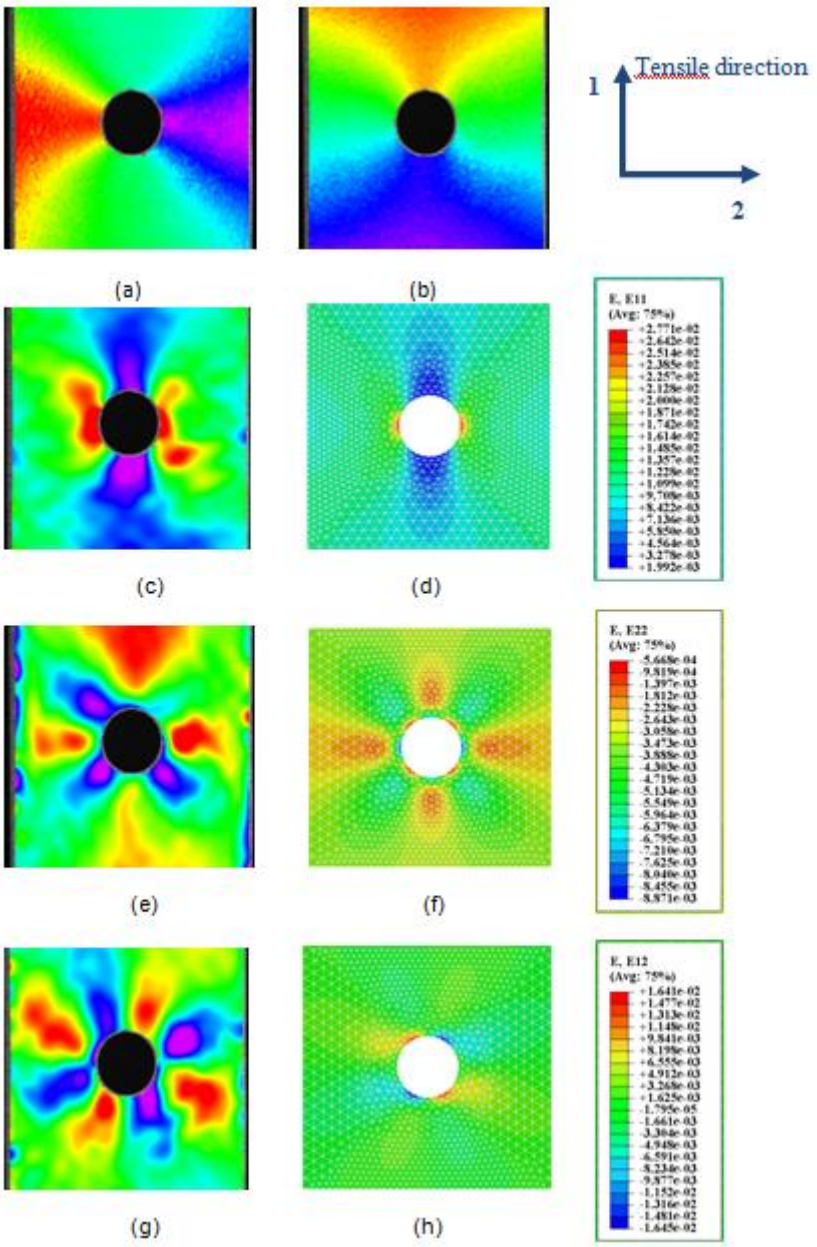

Figure 3. (a) Displacement field direction 2, (b) Displacement Field direction 1, (c) Experimental strain field Epsilon 11, (d) Numerical strain field Epsilon 11, (e) Experimental strain field Epsilon 22, (f) Numerical strain field Epsilon 22, (g) Experimental strain field Epsilon 12, (h) Numerical strain field Epsilon 12.

Image correlation shows heterogeneous deformation fields (ε_{xx} , ε_{yy} , ε_{xy}) . These strain fields do not exhibit symmetry; this is due to the distribution of glass fibers which is strongly heterogeneous in the specimen. Indeed, the injection gate is at the bottom left side of the sample and because the hole plays the role of an obstacle during injection and then induced a complex flow distribution.

The numerical strain fields are obtained by finite element simulation using Abaqus. The local stiffness matrix is evaluated according to the local orientation tensor predicted by injection simulation using moldflow software contained in the work of Y. Marco et al [3].

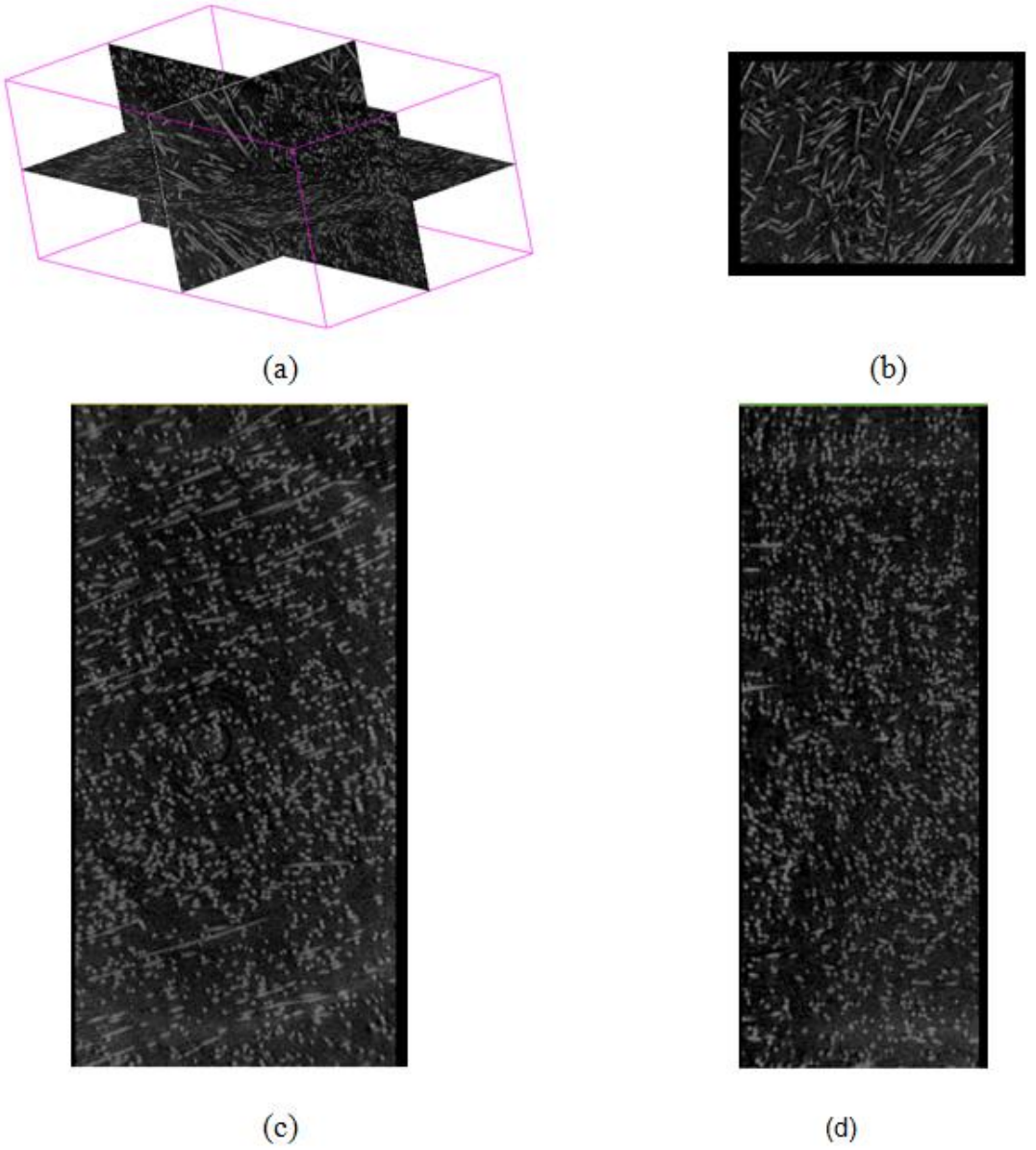

Figure 4. (a) Short Glass Fiber orientation in the thickness for the notched sample in the part of sample. , (b) distribution of glass fiber in central layer, (c) distribution of short glass fiber in the thickness X-direction, (d) distribution of short glass fiber in the thickness Y-direction.

In the modeling zone which is far from the injection gate, the orientation tensor field is quasi symmetric according the vertical plane of symmetry of the hole and then lead to a symmetric field of the local stiffness matrix field.

However, DIC shows a heterogeneous strain field around the hole and macroscopic crack initiates and propagates on the right side of the hole opposite of injection gate side. In the same manner bottom side and top side of the hole show a non symmetry of the strain field it is expected because the topic side should correspond to a weld line during injection.

That's why for a predictive simulation results, i.e. corresponding to the experimental results, we must consider the distribution of glass fibers in the thickness in different areas of the sample. In this sense, the X-ray tomography study is launched. Preliminary results show a variability in short glass fiber distribution in the thickness of the sample, and different areas

can be distinguished with a variability of layers in the number and layer thickness and different orientation of the short glass fibers.

The results of X-ray tomography are currently operating to launch a new simulation of damage evolution. This simulation is based on different number of layers, depending on the zone of sample and on the thickness, and depending on the different orientation of short glass fiber.

A study at meso scale is being developed to simulate the evolution of the damage in the automotive parts and structures based on the distribution of short glass fibers obtained by X-ray tomography.

Acknowledgement

The authors gratefully acknowledge the International Campus on Safety and Intermodality in Transportation (CISIT), the Nord-Pas-de-Calais Region and the European Community (FEDER funds) for partly funding the X-ray tomography equipment.

References

[1] H. Nouri, F. Meraghni, P. Lory. Fatigue damage model for injection-molded short glass fiber reinforced thermoplastics. *International Journal of Fatigue* (31): 934-942, 2009.

[2] F. Meraghni, CJ. Blakeman ML. Benzeggah. Effect of interfacial decohesion on stiffness reduction in random discontinuous fiber composites containing matrix microcracks. *Composite Science and Technology*;(56(5)):541–55, 1996.

[3] Y. Marco, V. Le Saux, L. Jégou, A. Launay, L. Serrano, I. Raoult, S. Calloch . Dissipation analysis in SFRP structural samples : thermomechanical analysis and comparison to numerical simulations. *International Journal of Fatigue*, 2014.

[4] M.F. Arif, N. Saintier, F. Meraghni, J. Fitoussi, T. Chemisky, G. Robert. Multiscale fatigue damage characterization in short glass fiber reinforced polyamide-66. *Composite: Part-B*, (61): 55-65, 2014.

[5] K.L. Reifsnider, Z. Gao A micromechanics model for composite under fatigue loading. *International Journal of Fatigue* 1991;13:149–56.

[6] S. Subramanian, K.L. Reifsnider,W.W. Stinchcomb. A cumulative damage model to predict the fatigue life of composite laminates including the effect of a fiber–matrix interphase. *International Journal of Fatigue* 1995;17:343–51.

[7] W. Van Paepegem, J. Degrieck A new coupled approach of residual stiffness and strength for fatigue of fiber-reinforced composites. *International Journal of Fatigue* 2002; 24:747–62.

[8] P. Ladevèze, E. Le Dantec, Damage modelling of the elementary ply for laminated composites. *Composite Science and Technology* 1992; 43:257–67.